

Correlation between Bax overexpression and prion deposition in medulla oblongata from natural scrapie without evidence of apoptosis

Jaber Lyahyai · Rosa Bolea · Carmen Serrano · Eva Monleón · Carlos Moreno · Rosario Osta · Pilar Zaragoza · Juan J. Badiola · Inmaculada Martín-Burriel

Received: 7 February 2006 / Revised: 31 May 2006 / Accepted: 31 May 2006 / Published online: 28 June 2006
© Springer-Verlag 2006

Abstract Although apoptosis has been implicated in the neuronal loss observed in prion diseases, the participation of apoptosis-related factors, like the Bcl-2 family of proteins, is still not clear. Moreover, there are conflicting data concerning the major role of apoptosis in the neuropathology associated with transmissible spongiform encephalopathies. Many studies have been developed in vitro or in experimentally infected animal models but, at present, little is known about this process in natural spontaneous and acquired prion diseases. In this work, the implication of Bax and Bcl-2 has been investigated by the analysis of their expression and protein distribution in medulla oblongata of naturally scrapie-infected sheep. Moreover, their spatial relationship with PrP^{Sc} deposition, neuronal vacuolation and neuropil spongiosis has also been analysed as well as the possible induction of neuronal apoptosis in this model. Real Time RT-PCR showed overexpression of the pro-apoptotic gene Bax in scrapie medullas, and immunohistochemistry confirmed its accumula-

tion. No variation of Bcl-2 was observed at the level of gene expression or protein production. Bax distribution, PrP^{Sc} deposition, neuronal vacuolation and spongiosis were quantified in different medulla oblongata nuclei and their spatial relationship was evaluated. Bax staining showed a positive correlation with prion deposition, suggesting that this factor is involved in prion neurotoxicity in our natural model. Despite Bax overexpression, neuronal apoptosis was revealed neither by TUNEL nor by immunohistochemical detection of the activated form of caspase-3. This lack of apoptosis could be attributed to the relatively low number of neurons in this area or to the existence of neuroprotective mechanisms in medulla oblongata motor neurons.

Keywords Prion · Bax · Bcl-2 · Apoptosis · Scrapie

Introduction

Transmissible spongiform encephalopathies (TSEs) or prion diseases, which include Creutzfeldt–Jakob disease (CJD) in humans, bovine spongiform encephalopathy in cattle and scrapie in sheep and goats, are fatal neurodegenerative disorders caused by prions, a type of unconventional agent that targets the central nervous system (CNS) in mammals. The neuropathological features of prion diseases include the accumulation of PrP^{Sc}, an abnormal isoform of the cellular prion protein (PRP^C), spongiform changes, neuronal loss and gliosis ([26] for review). As in other neurodegenerative diseases caused by the accumulation of toxic proteins, neurons in TSEs appear to die via programmed cell death (PCD). Apoptosis has been implicated in the

J. Lyahyai · C. Serrano · R. Osta · P. Zaragoza · I. Martín-Burriel (✉)
Laboratorio de Genética Bioquímica (LAGENBIO),
Facultad de Veterinaria, Universidad de Zaragoza,
Miguel Servet 177, 50013 Zaragoza, Spain
e-mail: minma@unizar.es

R. Bolea · E. Monleón · J. J. Badiola · I. Martín-Burriel
Centro Nacional de Referencia de EETs,
Facultad de Veterinaria, Universidad de Zaragoza,
Miguel Servet 177, 50013 Zaragoza, Spain

C. Moreno
Mejora Animal, Facultad de Veterinaria,
Universidad de Zaragoza, Miguel Servet 177,
50013 Zaragoza, Spain

brain damage and neuronal loss observed in these diseases ([12, 16, 18, 28, 40] for review).

In addition to apoptosis, two other types of PCD characterized by the apparition of cytoplasmic autophagic vacuoles and the formation of large empty spaces within the cytoplasm could be linked with the “spongiform vacuoles” observed in TSEs, as previously suggested [26, 40]. However, of these, only the molecular mechanisms of apoptosis are relatively well characterized. In vitro studies using synthetic peptides homologous to PrP have demonstrated the induction of apoptosis via the disruption of mitochondrial membrane, release of cytochrome *c* (hereafter, Cyt-*c*) and caspase activation [31]. This pathway is regulated by the expression of the proto-oncogene Bcl-2 family including the anti-apoptotic Bcl-2 gene and the pro-apoptotic Bax gene ([5] for review).

Several findings indicate functional interactions between PrP^C and Bcl-2. First, the N-terminal PrP region, which includes octapeptide repeats, shares a similarity with the Bcl-2 homology domain 2 (BH2) of these proteins [2, 43]. Second, neuronal cultures treated with PrP synthetic peptides down-regulate the expression of Bcl-2, the neuroprotective family member [13, 31]. Furthermore, overexpression of the Bcl-2 protein can attenuate the susceptibility of PrP^{-/-} neurons to the cell death induced by serum removal [25]. The vulnerability of cells to apoptosis in prion infection in vitro models is mediated by an increase of Bax expression and the activation of caspase-dependent apoptotic pathways in mitochondria [22]. Moreover, the cellular form of PrP can prevent Bax-mediated cell death in vitro [6, 35]. Nevertheless, in vivo investigations show contradictory results. Whereas decreased Bcl-2 and increased Bax expression is observed in scrapie-infected hamsters [32], no change in the levels of these proteins is detected in murine scrapie models [38]. In the sporadic form of CJD, both proteins are overexpressed in Purkinje cells from diseased patients [33]. Consequently, the possible role of these regulatory proteins in prion-associated neuropathology is unclear and to date, little is known regarding their activity in naturally acquired prion diseases. In order to shed light on this, we have analysed the modifications of the transcription levels of Bax and Bcl-2, as well as their protein distribution in the medulla oblongata region of naturally infected sheep. The division of medulla oblongata in well-delimited nuclei has allowed the study of the topological relationship between these two proteins and PrP^{Sc} accumulation, spongiosis and vacuolation. Finally, we have investigated their possible relationship in apoptosis induction in this area.

Methods

Animals

A total of 14 Rasa Aragonesa female sheep (aged 3–5 years) were included in this study. Nine of them exhibited clinical signs of scrapie in a terminal state. The diagnosis was confirmed using a rapid test and immunohistochemistry to detect PrP^{Sc} [4]. These animals belong to a flock of sheep, conserved for research purposes by the Spanish National Reference Centre for TSEs and where several scrapie cases have appeared in the last 4 years. Animals from this flock were genotyped for PRNP polymorphisms [1], and sheep chosen for this study displayed the ARQ/ARQ genotype. This naturally scrapie-infected flock is free from Brucella and Maedi-Visna and is periodically vaccinated against enterotoxemia caused by *Clostridium perfringens* and antiparasitary treatment. Control animals ($n = 5$) were selected from a different flock belonging to the same breed, where no scrapie had been reported to date. All animals were 3 to 5-year-old females with an identical PRNP genotype (ARQ/ARQ).

Necropsy and tissue collection

Necropsy was performed immediately after killing the animal, by intravenous injection of sodium pentobarbital and exsanguination. There were no other pathological signs upon physical examination of scrapie and control animals. One half of medulla oblongata from each sheep was taken and placed in RNA later (Ambion) for RNA analysis. The remaining half was fixed in 10% buffered formalin, post-fixed and embedded according to standard procedures. Medulla oblongata was chosen as the target tissue due to its highly structured neuronal system in nuclei. This structure allows the possibility of scoring both immunostained tissue and histopathological lesions for each nucleus and to analyse any relationship between markers.

Total RNA isolation and cDNA synthesis

Total RNA from half of the medulla oblongata was isolated using the RNeasy Mini Kit (Qiagen, Crawley, UK) following the manufacturer's instructions. In order to avoid contamination with genomic DNA, samples were treated for 15 min with 10 U of RNase-free DNase (Qiagen) at room temperature. The quality of the RNA was assessed based on the demonstration of distinct intact 28S and 18S ribosomal RNA bands. Concentrations were determined by OD (260/280). cDNA was synthesized from 1 µg of each RNA using

random hexamers primers with the Superscript First Standard Synthesis System for RT-PCR (Invitrogen, Paisley, UK).

Design of PCR primers and TaqMan probes

The PCR primer and TaqMan probe sequences used for quantification of the genes encoding 18S rRNA, GAPDH, ACTB (β -actin), Bcl-2 and Bax are shown in Table 1. The primers amplify PCR products between 65 and 182 base pairs (bp) long, which is within the suggested range of 50–200 bp recommended by Applied Biosystems for the TaqMan assay. Quantitative PCR assays were designed using Primer Express 2.0 software (Applied Biosystems, Foster City, CA, USA) to select appropriate primer and probe sequences from known sheep or bovine sequences. Bax primers and probe were designed from the sheep cDNA sequence (AF163774). An alignment of the cDNA sequence with sheep genomic DNA, previously isolated from our laboratory and reported to the GenBank database (DQ323116), showed the exon–exon border. The exon–exon border was considered when designing the Bax probe to prevent the amplification of genomic DNA in the PCR reaction. GAPDH primers were designed from the sheep cDNA sequence (AF035421) after a BLAST search revealed the exon–exon junctions. Sequences for mRNA encoding 18S ribosomal RNA and Bcl-2 were obtained from GenBank accession numbers AF176811 and AY423861, respectively (exon–exon borders were not considered). Finally, a fragment from sheep ACTB expression was amplified using previously described primers [15]. In the last three cases, the absence of contaminating genomic DNA in the cDNA template was confirmed prior to quantification. Retrotranscription with and without

enzyme was developed to confirm the elimination of any remaining DNA.

Real Time quantitative PCR

Expression of Bax and Bcl-2 was quantified by Real Time quantitative PCR. GAPDH, ACTB and 18S rRNA are three of the most common housekeeping genes used as internal controls in the analysis of gene expression data. To improve normalization accuracy, the geometric mean of these three genes was used for calculation of the Normalization Factor (NF) to which all samples were normalized [41]. ACTB expression was evaluated as previously described [15]. The other PCR reactions were performed using the TaqMan assay. PCR amplification was performed in an ABI-Prism 7000 Sequence Detection System (PE Applied Biosystem). The reaction mixtures of Bax, Bcl-2, GAPDH and 18S rRNA, containing primers, probes, water and $2 \times$ TaqMan Universal PCR Master Mix (PE Applied Biosystem), were prepared and dispersed in a 96-well optical tube (PE Applied Biosystem). Finally, complementary DNA equivalent to 5 ng of total RNA was added to each well for the analysis of mRNA expression. The total volume for each reaction was 25 μ l. Amplification of cDNA by PCR was achieved with an initial 10 min activation and denaturation step at 95°C, followed by 40 cycles of 15 s at 95°C and 30 s at 60°C. Baseline and threshold for Ct calculation were set automatically with the ABI-Prism 7000 SDS software Version 1.1 or manually whenever necessary. To compare transcript levels between samples, a standard curve of cycle thresholds for serial dilutions of a cDNA sample was established and then used for the estimation of relative amounts of each gene. All RT-PCR reactions were run in duplicate.

Table 1 Primers (F: forward and R: reverse) and TaqMan probe (P) sequences for each gene analysed

Gene	Primer and probe sequences	Concentration (nM)	Size (bp)	Accession number
<i>Bax</i>	F: 5' TGAAGCGCATTGGAGATGAA 3'	900	182	AF163774
	R: 5' CTTGAGCACCAAGTTTGCTGG 3'	900		
	P: FAM-AGTAACATGGAGCTGCAGAGGATGATCGC-TAMRA	100		
<i>Bcl-2</i>	F: 5' TGGTGGAGGAGCTCTTCAGG 3'	300	65	AY423861 [29]
	R: 5' TCCGAACTCAAAGAAGGCCA 3'	300		
	P: FAM-ATGCGCCCCCAGTTCACCCC-TAMRA	150		
GAPDH	F: 5' TCCATGACCACTTTGGCATCGT 3'	300	70	AF035421
	R: 5' GTCTTCTGGGTGGCAGTGA 3'	300		
	P: VIC-AGGGACTTATGACCACTGTCCACGCC-TAMRA	150		
18S rRNA	F: 5' GGAATCAGGGTTCGATTCC 3'	900	93	AF176811
	R: 5' GGGTCGGGAGTGCCTAATT 3'	900		
	P: FAM-TCCAAGGAAGGCAGCAGGCGC-TAMRA	150		

Primers and probe final concentrations in the Real Time PCR reaction mix, size of the fragment amplified and GenBank accession are also given

Immunostaining for apoptosis markers

Five micrometre paraffin-embedded sections from medulla oblongata of scrapie ($n = 9$) and control ($n = 5$) animals were prepared and processed for immunostaining of apoptosis markers. Different pre-treatment protocols were used depending on the marker studied. For Bcl-2, after deparaffinizing and rehydrating the tissue sections, the slides were immersed in a 4 $\mu\text{g/ml}$ proteinase K, 0.1% Tween 20, 0.05 M Tris and 8 mM EDTA buffer and incubated at 37°C for 15 min. The unmasking protocol used for active caspase-3 immunostaining included a steam heat procedure. In brief, rehydrated slices were immersed in pre-heated antigen retrieval solution (buffer citrate 1 \times , DAKO, Glostrup, Denmark), exposed to heat in a pressure cooker for 10 min and cooled slowly for 20 min. Pre-treatment was unnecessary for Bax immunostaining. After treatments, the sections were incubated with blocking reagent (DAKO) for 10 min to block endogenous peroxidase activity. Next, sections were incubated for 1 h at RT with one of the following primary antibodies: Bcl-2 (1:200; rabbit polyclonal; Upstate); Bax (1:300; rabbit polyclonal P-19; Santa Cruz) and Caspase-3 (1:40; mouse monoclonal Ab-4; Calbiochem). The enzyme-conjugated polymer Envision (DAKO, 30 min) was used as the visualization system and DAB (DAKO, 10 min) as chromogen. Sections were counterstained by treatment with haematoxylin.

Antibodies against Bax and Bcl-2 proteins were selected due to their previously established reactivity in formalin-fixed and paraffin-embedded sheep tissues [11]. The reactivity of both antibodies was confirmed in sheep lymph node tissue sections and the specificity of Bax staining was demonstrated by the elimination of labelling, after antiserum neutralization using excess of blocking peptide (Santa Cruz sc-526p). Moreover, the labelling of apoptotic lymphocytes in sheep lymph node sections confirmed the preferential reaction of anti-caspase-3 antibody against the activated form. A complete absence of labelling was obtained by omitting primary antibody in all cases. In routine immunoreactions, sheep lymph node tissue sections were included as positive controls whereas the omission of primary antibodies served as negative controls.

Histology and prion immunohistochemical detection

An anatomopathological study of medulla oblongata was performed in haematoxylin–eosin stained slices (one from each individual control and positive animal). Neuronal vacuolation and neuropil spongiosis were

evaluated in these stained sections as described below. Prion protein detection was performed in adjacent sections following pre-treatment as previously described [19]. Briefly, sections were pre-treated with 98% formic acid and hydrated, autoclaving to enhance antigen retrieval. After proteinase K digestion (4 $\mu\text{g/ml}$), the sections were incubated with blocking reagent (DAKO) for 10 min to block endogenous peroxidase activity. Next, sections were incubated with the monoclonal primary antibody L42 (R-Biopharm, Darmstadt, Germany; dilution 1:500) at RT for 30 min. Sections were processed with endogenous peroxidase blocking, visualization system and counterstaining following the previously described procedure for the detection of apoptosis markers.

Histochemical detection of apoptosis

In situ nick-end labelling was carried out using Apoptag[®] Plus Peroxidase In Situ Apoptosis Detection Kit (Chemicon International, CA, USA) as described in the manufacturer's protocol. Counterstaining was achieved by haematoxylin treatment. Sections from each medulla oblongata ($n = 14$) were analysed using this methodology. Sheep node lymph tissue sections were used as positive controls.

Data analysis

Histology and immunostaining were evaluated in seven medulla oblongata areas: hypoglossal motor nucleus, nucleus of solitary tract, nucleus of spinal tract of trigeminal nerve, medial cuneate nucleus, olivary nucleus, parasympathetic nucleus of vagus nerve and reticular formation. Intraneuronal vacuoles and neuropil spongiosis were scored on a scale of 0–3: 0, no neuron/neuropil vacuolation; 1, low; 2, medium; and 3, strong vacuolation or spongiosis in the whole nucleus or region. PrP^{Sc} and staining of apoptosis markers were measured in neurons and neuropil using the same subjective scoring where a score of 0 indicates no staining; 1 few stained cells; 2 intermediate; and 3, numerous stained cells. The subjective scores were carried out by two observers.

Statistic analysis

The relative differences in Bax and Bcl-2 gene expression between scrapie and control groups were defined as relative quantities after normalization with the NF. Quantitative results are expressed as mean \pm standard error of mean (SEM) values and the relative differences between groups were calculated and defined as relative increases, setting the control means at 100%.

Student's *t* test analysis was applied to determine whether the differences observed between groups were statistically significant ($P < 0.05$).

Immunostaining differences between control and scrapie medullas were determined using the unpaired non-parametric Mann–Whitney test. Moreover, the effect of area in immunostaining scores was evaluated by means of the non-parametric ANOVA Kruskal–Wallis test. The Mann–Whitney test was subsequently performed to determine any observed differences. Furthermore, the relationship between histological and immunohistochemical parameters was measured in scrapie-positive sheep using the non-parametric Spearman correlation. For the calculation of each correlation value, 40–63 data pairs, corresponding to the immunostaining and histopathological lesion scores in the seven oblongata medulla areas from the nine scrapie-positive sheep, were used.

Finally, to confirm the possibility of a direct relationship between Bax staining and intraneuronal vacuolation, neurons in the parasympathetic nucleus of vagus nerve and hypoglossal motor nucleus were counted taking into account these parameters, and a chi-square test was applied to determine their significance.

Results

Expression and distribution of Bax and Bcl-2 in scrapie medulla oblongata

The effect of prion infection on the ratio Bax/Bcl-2 was analysed in oblongata medullas from naturally scrapie-infected sheep. First, the relative expression of the Bax and Bcl-2 genes in medullas from control and scrapie sheep was determined by Real Time RT-PCR. Samples treated and untreated with retrotranscriptase showed differences of higher than 8 cycles in the amplification curves for Bcl-2 and 18S rRNA genes, indicating that genomic DNA was successfully removed (data not shown). Standard curves for Bax, Bcl-2, GAPDH, ACTB and 18S rRNA had the appropriate slopes (-3.91 , -3.69 , -3.89 , -3.07 and -3.32 , respectively) and correlation values ($r^2 > 0.97$, > 0.99 , > 0.99 , > 0.99 and > 0.99 , respectively). Bax transcripts were significantly increased in the scrapie group ($P < 0.05$). On the other hand, the means of Bcl-2 were similar in scrapie and control medullas (see Fig. 1).

The distribution of Bax and Bcl-2 proteins was examined in situ. Medulla oblongata specimens from clinical scrapie sheep and matched controls were studied and staining was quantified for the different areas. A dramatic overexpression of Bax was observed in the

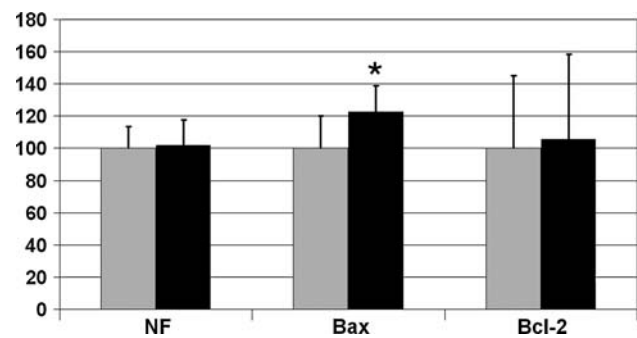


Fig. 1 Expression of Bax and Bcl-2, in control (grey bar, $n = 5$) and scrapie animals (black bar, $n = 5$) normalized to NF (Normalization Factor). Quantities are expressed as percentage of controls. Significant differences were detected using Student's *t* test ($*P < 0.05$)

neuronal perikaryon of specific neurons from scrapie medullas whereas it was minimally detected or undetected in other neurons (Fig. 2a). In contrast, neurons from controls revealed no staining in most cases (Fig. 2b). The antibody concentration used in the immunohistochemical reaction allowed the identification of cells overexpressing Bax, whereas basal levels of this protein were not detected. The quantitative rate (mean rank) of Bax intraneuronal staining in scrapie animals was significantly higher than that observed in the control group (Mann–Whitney *U* test $P < 0.001$), in agreement with the Bax mRNA expression results. The non-parametric Kruskal–Wallis test did not reveal a significant effect of area ($P = 0.766$) in Bax distribution, i.e. areas displaying the highest neuronal Bax immunoreaction scores were different in each animal. Figure 3 shows the homogeneity of mean ranks for Bax staining in different nuclei. In neuropil, Bax was observed to be weakly labelled in scrapie and control-matched animals without significant differences between the two.

No modification in the expression of Bcl-2 protein was detected in naturally scrapie-infected sheep, in accordance with transcript quantification. This marker revealed a homogeneous and diffuse immunostaining in every animal analysed (data not shown).

PrP^{Sc} deposition and scrapie histopathological lesions

Immunohistochemical determination of PrP^{Sc} accumulation confirmed the diagnosis of scrapie in sheep that presented neurological symptoms. Immunoreactivity for the protease-resistant form of PrP was negative in control animals. The intraneuronal and neuropil accumulation of prion protein was quantified for each area. The highest mean rank value for PrP intraneuronal staining was observed in the parasympathetic nucleus

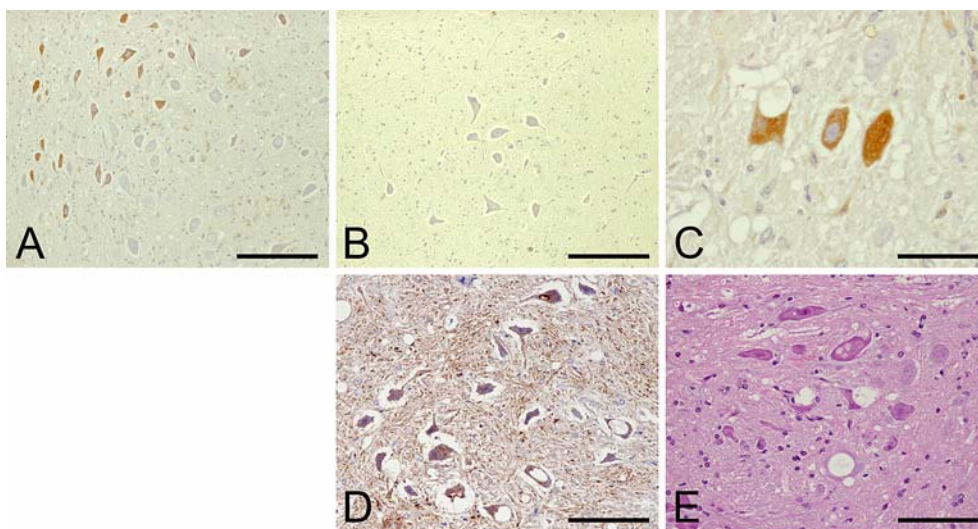


Fig. 2 **a** Bax immunostaining in the neuronal perikaryon of scrapie medullas (Bar, 250 μ m). **b** No intraneuronal Bax staining in controls (Bar, 250 μ m). **c** Cytoplasmic Bax immunostaining in vacuolized and non-vacuolized neurons (Bar, 50 μ m). **d** PrP^{Sc}

accumulation in medulla oblongata from scrapie animals (Bar, 100 μ m). **e** H–E stained section showing neuronal vacuolation and neuropil spongiosis in a scrapie medulla (Bar, 100 μ m)

of vagus nerve (Fig. 3a) and Kruskal–Wallis test revealed an effect of area with a significance of $P = 0.079$. The area effect was also observed in PrP^{Sc} distribution in neuropil ($P < 0.001$). In this case, areas showing the highest immunoreactivity were: parasympathetic nucleus of vagus nerve, tractus solitari and spinal tract of trigeminal nerve (Fig. 3b).

Intracytoplasmic neuronal vacuolation was observed only in the nucleus of vagus nerve, cuneatus and reticular formation; no significant differences were observed between these areas. Finally, neuropil spongiosis was high in the nucleus of vagus nerve and solitary tract. Because of this histopathological feature, the area effect was very significant (Kruskal–Wallis test $P < 0.01$) and significant differences were observed between high- and low-score groups (Mann–Whitney test $P < 0.01$). Figure 3a shows the mean ranks obtained for neuronal vacuolation in each area analysed and the values for neuropil spongiosis are depicted in Fig. 3b. Representative PrP^{Sc} immunostaining and H–E sections showing neuronal vacuolation and neuropil spongiosis are shown in Fig. 2d, e.

Correlation between Bax immunostaining and PrP^{Sc} deposition and other scrapie histopathological features

Immunodetection of Bax made it possible to determine any relationship focal increases of this pro-apoptotic marker might have with prion infection events. Intraneuronal Bax scores showed a significant Spearman correlation with PrP^{Sc} deposition in neurons ($r_s = 0.429$; $P < 0.01$) and neuropil ($r_s = 0.297$; $P < 0.05$).

A possible effect of PrP^{Sc} deposition in Bax staining was investigated by performing a Kruskal–Wallis test. The effect of intraneuronal accumulation of PrP^{Sc} in Bax expression was corroborated ($P < 0.01$). At low PrP^{Sc} levels, Bax staining remained steady, then reached a peak and declined in the greatest prion deposition score. The mean rank value obtained for Bax staining in the intermediate level of neuronal PrP^{Sc} deposition (value 2) was significantly different from the values observed for the other PrP^{Sc} scores ($P < 0.05$ for Mann–Whitney test). Figure 4 shows Bax mean rank values for each neuronal PrP^{Sc} staining category. The effect of neuropil PrP^{Sc} deposition in neuronal Bax expression, analysed by the non-parametric Kruskal–Wallis test, had a significant P value of 0.093.

Bax immunoreaction also showed a positive correlation with neuronal vacuolation ($r_s = 0.362$; $P < 0.05$). A contingency table and chi-square test were performed in order to investigate if this correlation was due to sharing the same anatomical area or a role for Bax in the vacuolation process. A total of 1,189 neurons were counted in the parasympathetic nucleus of vagus nerve and hypoglossal motor nucleus of scrapie animals ($n = 9$), and a chi-square test revealed that Bax induction and neuronal vacuolation occurred as two independent phenomena.

Neuronal apoptosis in medulla oblongata of scrapie animals

The TUNEL method was employed to determine apoptosis in medulla oblongata. Glial-positive nuclei

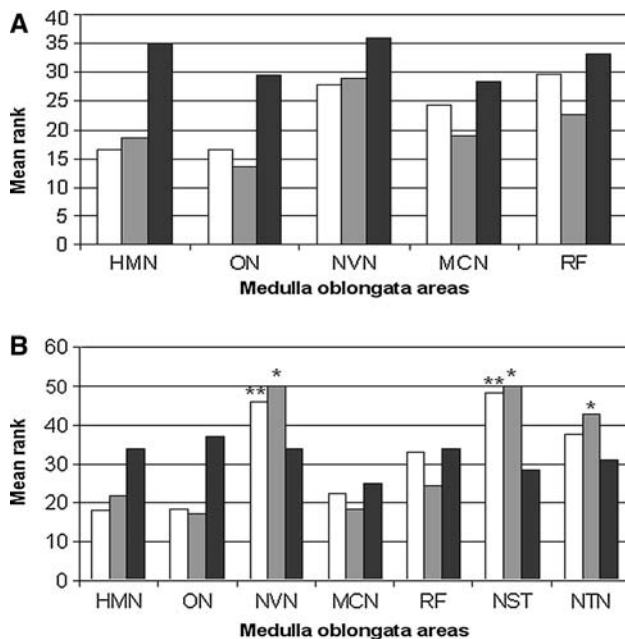


Fig. 3 Mean rank values for: **a** neuronal vacuolation (white bar), PrP^{Sc} intraneuronal deposition (grey bar) and neuronal Bax staining (black bar) in different medulla oblongata areas from scrapie animals. **b** Neuropil spongiosis (white bar), PrP^{Sc} deposition (grey bar) and Bax immunostaining (black bar) in neuropil of medulla oblongata from scrapie animals. Medulla oblongata areas analysed: hypoglossal motor nucleus (HMN), olivary nucleus (ON), parasympathetic nucleus of vagus nerve (NVN), medial cuneate nucleus (MCN), reticular formation (RF), nucleus of solitary tract (NST) and nucleus of spinal tract of trigeminal nerve (NTN). *These areas showed significant differences (Mann–Whitney test $P < 0.05$) with the others. **Areas showing significant differences (Mann–Whitney test $P < 0.01$) with HMN, ON and MCN

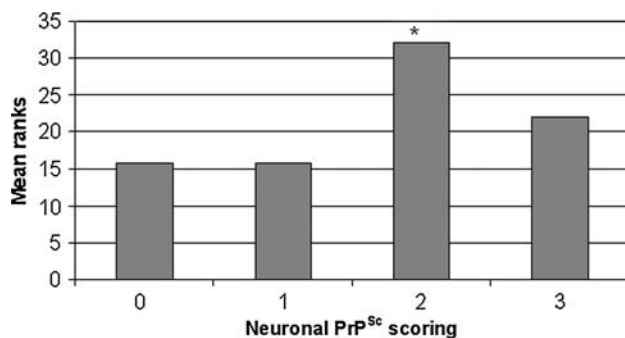


Fig. 4 Bax immunostaining mean rank values for each intraneuronal PrP^{Sc} category (X-axis). Kruskal–Wallis significance ($P < 0.01$). *Bax mean rank for PrP^{Sc} category 2 was significantly higher than mean ranks for the other categories (Mann–Whitney test $P < 0.05$)

were observed in both scrapie and control sections (see Fig. 5a), although the number of stained nuclei was too low for a statistical comparison. TUNEL staining was not observed in neuronal nuclei, either in scrapie or in control animals.

Cell death was also analysed by immunodetection of the activated form of caspase-3. Medulla oblongata sections of scrapie and control sheep were stained using an antibody, which preferentially reacts with the activated form of caspase-3. Neurons containing activated caspase-3 did not display the typical morphological features of apoptosis (shrunken, condensed or fragmented nuclei and cytoplasm). Cytoplasmic staining was detected in motoneurons from seven scrapie and three control animals (Fig. 5b). Caspase-3 neuronal immunostaining was not significantly different in scrapie and control groups and was not correlated with PrP^{Sc} deposition and scrapie-associated lesions. Apart from neurons, apoptotic white matter cells were immunoreactive to activated caspase-3 in both scrapie and controls. In addition to cells exhibiting an apoptotic morphology (Fig. 5c), caspase-3 staining was observed in apparently healthy cells, where immunoreactivity appeared as a granular pattern (Fig. 5d).

Discussion

Although apoptosis has been implicated in the neuronal loss observed in prion diseases [12, 16, 18, 28, 40], there are contradictory findings with respect to the participation of certain apoptotic molecules in this process in vivo [32, 33, 38], as well as in the major role of this process in neuronal death [17, 21]. The first aim of the present study was to analyse the implication of Bax and Bcl-2 in the neuropathology associated with acquired TSEs using naturally scrapie-infected sheep as a natural model of these diseases. Next, their relationship with prion deposition, neuronal vacuolation and neuropil spongiosis was also investigated. Our final goal was to determine if the induction of the pro-apoptotic molecule Bax was associated with an increase in apoptosis.

In our natural animal model, the ratio of pro- and antiapoptotic genes Bax and Bcl-2 was modified in scrapie due to the overexpression of the former. Both mRNA analysis and immunodetection of Bax were in accordance with the findings observed in vitro [22] and in experimental scrapie infection in hamsters [32]. Moreover, as Bax induction was also observed in Purkinje cells of spontaneous Creutzfeldt–Jakob cerebella [33] our results confirm the induction of this molecule in natural prion diseases, independent of the area analysed. The correlation observed between Bax staining and PrP^{Sc} deposition suggested that Bax is involved in the mechanisms of prion neurotoxicity in oblongata medulla from naturally infected sheep. The existence of apparently different populations of Bax-immuno-

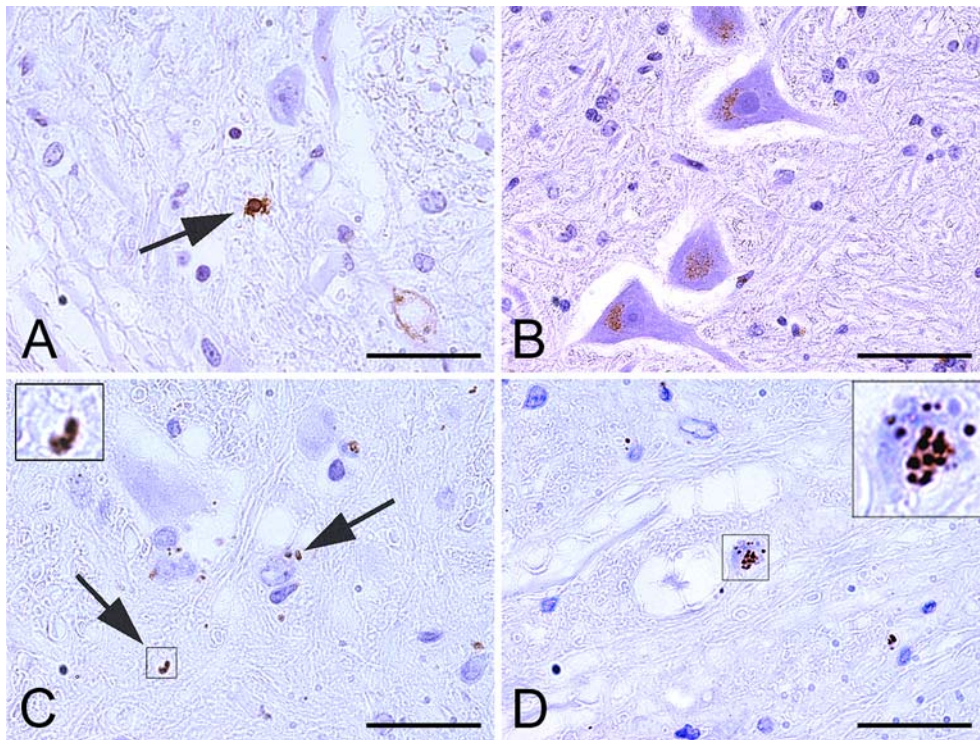


Fig. 5 **a** Arrow shows a glial nucleus stained with TUNEL in the medulla oblongata of a scrapie animal (Bar, 31.5 μ m). **b** Neuronal cytoplasmic staining for the active form of caspase-3 observed in a scrapie medulla (Bar, 31.5 μ m). **c** Arrows show active caspase-3

staining in the cytoplasm of a glial cell with apoptotic morphology (Bar, 31.5 μ m). **d** Granular active caspase-3 immunostaining in apparently healthy glial cells (Bar, 31.5 μ m). The areas selected are magnified $\times 3$

reactive neurons in the same nuclei, when prion deposition is homogeneously distributed, could be attributed to the presence of cells in different stages of the neurotoxic process. In an *in vivo* model, we would not expect to observe synchronicity across the cells.

As shown in Fig. 4, it seems that a threshold exists from which accumulation of PrP^{Sc} becomes toxic. This threshold has also been described for the apparition of neuropathological lesions in a genetic TSE mouse model [10]. At low levels of PrP^{Sc}, the non-pathological form PrP^C could exercise its protective action, avoiding the up-regulation of Bax. This action could be related to the role proposed for PrP^C in the cell's response to oxidative stress ([7, 40] for reviews), as an increase of Bax levels is linked to this process in cultured neurones [30, 34, 37] and recently, the implication of oxidative stress in the pathogenesis of spontaneous CJD had been suggested [14]. On the other hand, the decrease of Bax observed in the highest level of PrP^{Sc} could be a consequence of the progress in the neurodegeneration associated with this disease.

Does the increase of Bax imply an activation of the apoptotic pathway in natural scrapie? In our study, neither TUNEL nor active caspase-3 immunostaining

confirmed the presence of neuronal apoptosis in medulla oblongata of naturally infected scrapie animals. The absence of TUNEL-positive neurons could be expected as only a few neurons are expected to die at a given time point in a chronic disease like natural scrapie. What is observed may present a minute proportion of all apoptotic events going on in TSE-affected brains.

However, *in vitro* and *in vivo* models of prion diseases have shown the activation of caspase-3 [9, 20, 38, 42] and its determination has also successfully been employed to identify apoptotic neurons in other chronic neuropathologies such as Alzheimer's disease [39], although in exceptionally low numbers. In our study, the active form of caspase-3 was observed in neuron cytoplasm of scrapie and control medullas, in a very low number of cells in both groups and with a focal and weak staining pattern. Moreover, stained neurons did not exhibit an apoptotic appearance. These findings prevented us from concluding that neuronal apoptosis is present in scrapie medullas.

Two hypotheses could explain the absence of this PCD: first, the existence of a very low level of apoptosis in this area and second, the arrest of apoptosis after

Bax induction. In accordance with the former, several experiments have shown that the highest density of apoptotic cells has been observed in those neuroanatomical areas in which spongiform changes are minimal or absent, such as retina and cerebellum granular layer ([24, 26] and unpublished results from our group in natural scrapie infected sheep cerebellum), and medulla oblongata is considered as a scrapie diagnosis target tissue due to the high presence of PrP^{Sc}, neuronal vacuolation and spongiosis changes. Moreover, in other neurodegenerative disease models, such as the familiar ALS transgenic mice, vacuolation in motoneurons is not related to apoptotic nuclei either [3]. Thus, vacuolation could be linked to other types of PCD such as autophagy [26]. On the other hand, this lack of apoptosis could also be related to the number of neurons, whereas there is a high density of neurons in retina and cerebellum granular layer, medulla oblongata nuclei are composed of a relative low number of neurons, and the probability of finding an apoptotic cell is much more reduced.

With respect to the second hypothesis, the overexpression of Bax without induction of apoptosis has been reported in vitro in a tumorigenic epithelial cell line [27], and in cerebellar Purkinje cells of CJD patients the overexpression of this pro-apoptotic molecule was not lethal either [33]. In our in vivo model, we were unable to detect apoptosis in Purkinje cells (unpublished results). An arrest of the mitochondrial apoptotic pathway could be executed at different moments, from the impediment of the Bax pro-apoptotic conformational change initially after Bax activation, similar to the cellular prion protein [36], or to the prevention of the caspase cascade, attributed to heat shock proteins [8]. The accumulation of these proteins has been observed in Purkinje cells in CJD [23] and may be part of a cytoprotective mechanism. Therefore, we cannot reject the possible existence of neuroprotective mechanisms against prion toxicity in specific neuronal populations such as medulla oblongata motor neurons or cerebellum Purkinje cells.

In summary, we have detected a correlation between the overexpression of Bax and PrP^{Sc} deposition in the absence of neuronal apoptosis in medulla oblongata of naturally acquired scrapie. Further investigations analysing other CNS areas, as well as other molecular factors involved in the mitochondrial pathway of apoptosis, will be necessary to elucidate the causes of this lack of apoptosis. Nevertheless, our results support the findings observed in other natural TSEs as the sporadic form of CJD, making naturally infected scrapie sheep a good animal model for the investigation of sporadic prion diseases.

Acknowledgments The authors thank Nuria Segovia and Silvia Ruiz for their technical assistance. This work was performed as part of the EET2003-09890 project (CICYT/FEDER), Red CIEN (Carlos III Institute), Fondo de Investigación Sanitaria (PI020840) and Research Consolidated Groups from the Aragon Government. J. Lyahyai and C. Serrano were supported by AEIC (MAE) and DGA doctoral grants, respectively, and I. Martín-Burriel by a research contract from the Ramón y Cajal Program.

References

- Acín C, Martín-Burriel I, Goldmann W, Lyahyai J, Monzón M, Bolea R, Smith A, Rodellar C, Badiola JJ, Zaragoza P (2004) Prion protein gene polymorphisms in healthy and scrapie-affected Spanish sheep. *J Gen Virol* 85:2103–2110
- Adams JM, Cory S (1998) Matters of life and death: programmed cell death at Cold Spring Harbor. *Science* 281:1322–1326
- Bendotti C, Calvaresi N, Chiveri L, Prella A, Moggio M, Braga M, Silani V, De Biasi S (2001) Early vacuolization and mitochondrial damage in motoneurons of FALS mice are not associated with apoptosis or with changes in cytochrome oxidase histochemical reactivity. *J Neurol Sci* 191:25–33
- Bolea R, Monleón E, Schiller I, Raeber A, Acín C, Monzón M, Martín-Burriel I, Struckmeyer T, Oesch B, Badiola JJ (2005) Comparison of immunohistochemistry and two rapid tests for detection of PrP^{Sc} in different brain regions of sheep with typical scrapie. *J Vet Diagn Invest* 14:467–469
- Borner C (2003) The Bcl-2 protein family: sensors and checkpoints for life-or-death decisions. *Mol Immunol* 11:615–647
- Bounhar Y, Zhang Y, Goodyer CG, LeBlanc A (2001) Prion protein protects human neurons against Bax-mediated apoptosis. *J Biol Chem* 276:39145–39149
- Brown DR (2005) Neurodegeneration and oxidative stress: prion disease results from loss of antioxidant defence. *Folia Neuropathol* 43:229–243
- Bruey JM, Ducasse C, Bonniaud P, Ravagnan L, Susin SA, Diaz-Latoud C, Gurbuxani S, Arrigo AP, Kroemer G, Solary E, Garrido C (2000) Hsp27 negatively regulates cell death by interacting with cytochrome c. *Nat Cell Biol* 2:645–652
- Carimalo J, Corner S, Petit G, Peyrin JM, Boukhtouche F, Arbez N, Lemaigre-Dubreuil Y, Brugg B, Miguel MC (2005) Activation of the JNK-c-Jun pathway during the early phase of neuronal apoptosis induced by PrP106-126 and prion infection. *Eur J Neurosci* 21:2311–2319
- Chiesa R, Drisaldi B, Quaglio E, Migheli A, Piccardo P, Ghetti B, Harris DA (2000) Accumulation of protease-resistant prion protein (PrP) and apoptosis of cerebellar granule cells in transgenic mice expressing a PrP insertional mutation. *Proc Natl Acad Sci USA* 97:5574–5579
- Colliti M, Stefanon B, Wilde CJ (1999) Apoptotic cell death, bax and bcl-2 expression during sheep mammary gland involution. *Anat Histol Embryol* 28:257–264
- Fairbairn DW, Carnahan KG, Thwaites RN, Gribbs RV, Holyoak GR, O'Neill KL (1994) Detection of apoptosis induced DNA cleavage in scrapie-infected sheep brain. *FEMS Microbiol Lett* 115:341–346
- Forloni G, Bugiani O, Tagliavini F, Salmona M (1996) Apoptosis-mediated neurotoxicity induced by beta-amyloid and PrP fragments. *Mol Chem Neuropathol* 28:163–171
- Freixes M, Rodríguez A, Dalfo E, Ferrer I (2006) Oxidation, glycoxidation, lipoxidation, nitration, and responses to oxidative stress in the cerebral cortex in Creutzfeldt-Jakob disease. *Neurobiol Aging* (in press)

15. García-Crespo D, Juste RA, Hurtado A (2005) Selection of ovine housekeeping genes for normalisation by real-time RT-PCR; analysis of PrP gene expression and genetic susceptibility to scrapie. *BMC Vet Res* 3:1746–6148
16. Giese A, Groschup MH, Hess B, Kretzschmar HA (1995) Neuronal cell death in scrapie-infected mice is due to apoptosis. *Brain Pathol* 5:213–221
17. Graeber MB, Moran LB (2002) Mechanisms of cell death in neurodegenerative diseases: fashion, fiction, and facts. *Brain Pathol* 12:385–390
18. Gray F, Chretien F, Adle-Biassette H, Dorandeu A, Ereau T, Deslise MB, Kopp N, Ironside JW, Vital C (1999) Neuronal apoptosis in Creutzfeldt-Jakob disease. *J Neuropathol Exp Neurol* 58:321–328
19. Hardt M, Baron T, Groschup MH (2000) A comparative study of immunohistochemical methods for detecting abnormal prion protein with monoclonal and polyclonal antibodies. *J Comp Pathol* 122:43–53
20. Jamieson E, Jeffrey M, Ironside JW, Fraser JR (2001) Activation of Fas and caspase 3 precedes PrP accumulation in 87V scrapie. *Neuroreport* 12:3567–3572
21. Jesionek-Kupnicka D, Kordek R, Buczynski J, Liberski PP (2001) Apoptosis in relation to neuronal loss in experimental Creutzfeldt-Jakob disease in mice. *Acta Neurobiol Exp (Wars)* 61:3–9
22. Kim BH, Lee HG, Choi JK, Kim JI, Choi EK, Carp RI, Kim YS (2004) The cellular prion protein (PrPC) prevents apoptotic neuronal cell death and mitochondrial dysfunction induced by serum deprivation. *Brain Res Mol Brain Res* 124:40–50
23. Kovács GG, Kurucz I, Budka H, Ádori C, Müller F, Ács P, Klöppel S, Schätzl HM, Mayer J, László L (2001) Prominent stress response of Purkinje cells in Creutzfeldt-Jakob disease. *Neurobiol Dis* 8:881–889
24. Kretzschmar HA, Giese A, Brown DR, Herms J, Schmidt B, Groschup MH (1996) Cell death in prion disease. In: Court L, Dodet B (eds) *Transmissible subacute spongiform encephalopathies: prion disease. Proceedings of the third international symposium on transmissible subacute spongiform encephalopathies: prion disease.* Vak-de-Grace, Paris, France/Elsevier, Amsterdam/Oxford, Paris, pp97–106 (cited by 28)
25. Kuwahara C, Takeuchi AM, Nishimura T, Haraguchi K, Kubosaki A, Matsumoto Y, Saeki K, Matsumoto Y, Yokoyama T, Itohara S, Onodera T (1999) Prions prevent neuronal cell-line death. *Nature* 400:225–226
26. Liberski PP, Sikorska B, Bratosiewicz-Wasik J, Gajdusek DC, Brown P (2004) Neuronal cell death in transmissible spongiform encephalopathies (prion diseases) revisited: from apoptosis to autophagy. *Int J Biochem Cell Biol* 36:2473–2490
27. Lin PH, Pan Z, Zheng L, Li N, Danielpour D, Ma JJ (2005) Overexpression of Bax sensitises prostate cancer cells to TGF- β induced apoptosis. *Cell Res* 15:160–166
28. Lucassen PJ, Williams A, Chung WC, Fraser H (1995) Detection of apoptosis in murine scrapie. *Neurosci Lett* 198:185–188
29. Lyahyai J, Goldammer T, Beattie AE, Zaragoza P, Martin-Burriel I (2005) Positional and functional characterisation of apoptosis related genes belonging to the BCL2 family in sheep. *Cytogenet Genome Res* 109:519–526
30. de la Monte SM, Chiche J, von dem Bussche A, Sanyal S, Lahousse SA, Janssens SP, Bloch KD (2003) Nitric oxide synthase-3 overexpression causes apoptosis and impairs neuronal mitochondrial function: relevance to Alzheimer's-type neurodegeneration. *Lab Invest* 83:287–298
31. O'Donovan CN, Tobin D, Cotter TG (2001) Prion protein fragment PrP 106–126 induces apoptosis via mitochondrial disruption in human SH-SY5Y cells. *J Biol Chem* 276:45516–45523
32. Park SK, Choi SI, Jin JK, Choi EK, Kim JI, Carp RI, Kim YS (2000) Differential expression of Bax and Bcl-2 in the brains of hamsters infected with 263 K scrapie agent. *Neuroreport* 11:1677–1682
33. Puig B, Ferrer I (2001) Cell death signalling in the cerebellum in Creutzfeldt-Jakob disease. *Acta Neuropathol (Berl)* 102:207–215
34. Ray SK, Fidan M, Nowak MW, Wilford GG, Hogan EL, Banik NL (2000) Oxidative stress and Ca²⁺ influx upregulate calpain and induce apoptosis in PC12 cells. *Brain Res* 852:326–334
35. Roucou X, Gains M, LeBlanc AC (2004) Neuroprotective functions of prion protein. *J Neurosci Res* 75:153–161
36. Roucou X, Giannopoulos PN, Zhang Y, Jodoin J, Goodyer CG, LeBlanc A (2005) Cellular prion protein inhibits proapoptotic Bax conformational change in human neurons and in breast carcinoma MCF-7 cells. *Cell Death Differ* 12:783–795
37. Shou Y, Li N, Li L, Borowitz JL, Isom GE (2002) NF- κ B-mediated up-regulation of Bcl-X(S) and Bax contributes to cytochrome c release in cyanide-induced apoptosis. *J Neurochem* 81:842–852
38. Siso S, Puig B, Varea R, Vidal E, Acin C, Prinz M, Montrasio F, Badiola J, Aguzzi A, Pumarola M, Ferrer I (2002) Abnormal synaptic protein expression and cell death in murine scrapie. *Acta Neuropathol (Berl)* 103:615–626
39. Stadelmann C, Deckwerth TL, Srinivasan A, Bancher C, Brück W, Jellinger K, Lassmann H (1999) Activation of Caspase-3 in single neurons and autophagic granules of granulovacuolar degeneration in Alzheimer's Disease. *Am J Pathol* 155:1459–1466
40. Unterberger U, Voigtländer T, Budka H (2005) Pathogenesis of prion diseases. *Acta Neuropathol* 109:32–48
41. Vandesompele J, De Preter K, Pattyn F, Poppe B, Van Roy N, De Paepe A, Speleman F (2002) Accurate normalization of real-time quantitative RT-PCR data by geometric averaging of multiple internal control genes. *Genome Biol* 3:research004.1–0034.12
42. White AR, Guirguis R, Braier MW, Jobling MF, Hill AF, Beyreuther K, Barrow CJ, Masters CL, Collins SJ, Cappai R (2001) Sublethal concentrations of prion peptide PrP106-126 or the amyloid beta peptide of Alzheimer's disease activates expression of proapoptotic markers in primary cortical neurons. *Neurobiol Dis* 8:299–316
43. Yin XM, Oltvai ZN, Korsmeyer SJ (1994) BH1 and BH2 domains of Bcl-2 are required for inhibition of apoptosis and heterodimerization with Bax. *Nature* 369:321–323